Journal of Magnetic Resonance 211 (2011) 37–44

Contents lists available at ScienceDirect

Journal of Magnetic Resonance

journal homepage: www.elsevier.com/locate/jmr

^{1}H assisted $^{13}C/^{15}N$ heteronuclear correlation spectroscopy in oriented sample solid-state NMR of single crystal and magnetically aligned samples

Eugene C. Lin, Stanley J. Opella *

Department of Chemistry and Biochemistry, University of California San Diego, 9500 Gilman Drive, La Jolla, CA 92035-0307, USA

ARTICLE INFO

Article history:
Received 6 February 2011
Revised 23 March 2011
Available online 9 April 2011

Keywords:
^{13}C NMR
Solid-state NMR
Oriented samples
Cross-polarization
Triple-resonance

ABSTRACT

^{1}H-irradiation under mismatched Hartmann–Hahn conditions provides an alternative mechanism for carrying out $^{15}N/^{13}C$ transfers in triple-resonance heteronuclear correlation spectroscopy (HETCOR) on stationary samples of single crystals and aligned samples of biopolymers, which improve the efficiency especially when the direct $^{15}N–^{13}C$ dipolar couplings are small. In many cases, the sensitivity is improved by taking advantage of the $^{13}C_{\alpha}$ labeled sites in peptides and proteins with ^{13}C detection. The similarities between experimental and simulated spectra demonstrate the validity of the recoupling mechanism and identify the potential for applying these experiments to virus particles or membrane proteins in phospholipid bilayers; however, further development is needed in order to derive quantitative distance and angular constraints from these measurements.

1. Introduction

Solid-state NMR spectroscopy is playing an increasingly important role in the determination of the structures of proteins in biological supramolecular assemblies, such as membrane proteins in phospholipid bilayers [1–4], coat proteins of virus particles [5], and aggregates of amyloid proteins [6]. Oriented sample (OS) solid-state NMR is particularly well suited to molecular assemblies that can be mechanically or magnetically [7] aligned in the field. This allows angular constraints to be derived from the measured frequencies relative to a single external axis, which fully defines the alignment tensor, unlike the situation for residual dipolar couplings (RDCs) in solution NMR where determination of the alignment tensor can be a major source of error [8]. Significantly, since each measurement is independent of the others any experimental errors in the measurements of frequencies or uncertainties in the magnitudes or molecular orientations of the spin-interaction tensors do not accumulate. This results in high-resolution and accurate structure determinations.

OS solid-state NMR has been successfully applied to DNA, membrane proteins, and viral coat proteins, primarily through the use of uniform and selective ^{15}N labeling. ^{15}N labeling of biopolymers has many advantages [9]. Uniform ^{15}N labeling is easy and inexpensive to implement by expressing the protein of interest in bacteria grown on chemically defined media where there is only a single source of nitrogen, typically a salt of ammonia. Since no nitrogens are directly bonded in biopolymers, and in the critical polypeptide backbone of proteins each amide nitrogen is separated from another by two carbon atoms and three bonds, homonuclear $^{15}N/^{15}N$ decoupling is not necessary at any stage of the experiments because of the combination of the low gyromagnetic ratio and spatial separation of nitrogen atoms. Many double-resonance $^{1}H/^{15}N$ experiments have been developed to measure frequencies from the three spin-interactions available at a single ^{15}N labeled site: ^{1}H chemical shift, ^{15}N chemical shift, and $^{1}H/^{15}N$ heteronuclear dipolar couplings [10–13]. A number of assignment schemes have been developed based on both through-space interactions and the regularity of structural and spectral features that accompany the mapping of the structure onto the spectra by the anisotropic spin-interactions in the secondary structures of the α-helix and β-sheet [14,15]. Recently, through-space methods of identifying proximate nuclei have been improved by invoking assistance from a third spin [16,17].

In order to further advance OS solid-state NMR methods, triple-resonance experiments on ^{13}C and ^{15}N double labeled samples are an essential next step. This would enable spectroscopic interrogation of essentially all sites in a biopolymer. Since all backbone sites of a protein would be labeled it offers the possibility of systematic assignment schemes, and with ^{13}C detection higher sensitivity. However, in fully labeled biomolecules there is a significant problem. The ^{13}C form a dense network of homonuclear dipole–dipole coupled nuclei that interfere with most multi-dimensional solid-state NMR experiments as well as ^{13}C detection. We have taken two approaches to ameliorating these difficulties. One is to use 'tailored' ^{13}C labeling through judicious choice of ^{13}C-containing precursors in the growth media [18]. This enables either uniform dilution of the ^{13}C nuclei or high levels of labeling at selected sites

* Corresponding author. Fax: +1 858 822 4821.
E-mail address: sopella@ucsd.edu (S.J. Opella).

1090-7807/$ - see front matter © 2011 Elsevier Inc. All rights reserved.
doi:10.1016/j.jmr.2011.03.020

where nearby carbons are unlabeled. The strong homonuclear dipole–dipole couplings are attenuated by the effect of the dilution on their spatial proximity. The second approach is to develop NMR experiments that incorporate homonuclear decoupling on both the ^{1}H and ^{13}C channels [19]. The implementation of triple-resonance experiments provides ^{13}C chemical shift, and ^{1}H–^{13}C angular constraints that complement those from ^{15}N especially since some of them are out of the peptide plane, and as a result add unique information to the structure calculations. Moreover, ^{13}C detection offers increased sensitivity compared to the corresponding ^{15}N detection.

Cross-polarization (CP) between abundant spins and dilute spins has been demonstrated successfully both in magic angle spinning (MAS) and stationary solid-state NMR experiments. The magnetization can be transferred from ^{1}H to either ^{15}N or ^{13}C easily because of the strong dipolar couplings, up to 11 kHz or 22 kHz in peptides, respectively. In the basic cross-polarization experiment introduced by Waugh and coworkers [20], the observed signals are enhanced by up to 10- or 4-fold for ^{15}N and ^{13}C, respectively [21]. Here we are interested in using these large initial increases in magnetization to enable subsequent transfers to provide additional frequency dimensions for resolution, and to initiate the development of systematic assignment methods for OS solid-state NMR.

The first goal of the pulse sequence is to transfer magnetization from the initially polarized dilute spin to the second type of dilute spin. In general, this is referred to as double-cross-polarization (DCP) [22], although the details of the spectroscopy can vary significantly among the pulse sequences used to carry out this procedure. In the simplest example, the magnetization can be transferred from ^{1}H to ^{15}N, and then from ^{15}N to ^{13}C; alternatively, the magnetization can be transferred from ^{1}H to ^{13}C, and then from ^{13}C to ^{15}N. In general, the efficiency of the magnetization transfer between dilute spins (^{15}N and ^{13}C) is low due to the relatively small dipolar couplings between these two nuclei, which are generally less than 1 kHz because of their relatively low gyromagnetic ratios.

Here we demonstrate that it is possible to obtain two-dimensional ^{13}C/^{15}N heteronuclear correlation (HETCOR) spectra for all directly bonded pairs of ^{15}N and $^{13}C_{\alpha}$ in the backbone of a peptide or protein. Ideally, we would like all of the correlation resonances to have equal intensity, however, for now we have to settle for reliable detection of the correlation resonances for all pairs of ^{15}N and $^{13}C_{\alpha}$ in the peptides or proteins. Since the input for the structure calculations is in the form of the orientationally-dependent frequencies, not intensities or line shapes, this is much less of a handicap than in other classes of experiments, such as spin-exchange where the intensities of the off-diagonal peaks are important.

Longer mixing times generally improve the extent of magnetization transfer, especially when the dipolar couplings are small. However, the longer mixing times can also result in non-selective magnetization transfer or spin diffusion, depending on the various laboratory and rotating relaxation times. For solid-state NMR of stationary samples, selective magnetization transfers between ^{1}H and ^{15}N or ^{1}H and ^{13}C are feasible when the homonuclear ^{1}H/^{1}H dipole–dipole couplings are strongly attenuated, allowing individual heteronuclear dipolar couplings to dominant during specified time intervals of multi-dimensional experiments. Polarization inversion spin exchange at the magic angle (PISEMA) [10], SAMMY [11], and related pulse sequences are able to decouple the homonuclear ^{1}H dipolar networks and selectively transfer the magnetization between ^{1}H and ^{15}N [23,24]. Alternatively, dipolar-based INEPT [25], also is effective for transferring magnetization when the ^{1}H network of homonuclear couplings is suppressed. However, during many trials, we were unable to obtain efficient magnetization transfer between ^{15}N and ^{13}C using this family of pulse sequences. In contrast, spin-lock on both ^{15}N and ^{13}C with matched continuous wave irradiation does transfer magnetization between coupled ^{15}N and ^{13}C sites.

Third-spin assisted polarization transfer (TSAR) has been proposed as a method to recouple dilute spins under MAS condition [26]. However, instead of spinning the sample, the offsets can be created under the mismatched Hartmann–Hahn conditions between the abundant and dilute spins [16,17] that effect recoupling in stationary solid-state NMR experiments, as shown in the following equation:

$$H_{\pm} = -\frac{1}{8\Delta\omega_I}\sum_{n=1}^{N} a_{1n}a_{2n}I_z^{(n)}(S_+^{(1)}S_-^{(2)} + S_-^{(1)}S_+^{(2)}) \tag{1a}$$

$$H_{II} = \frac{1}{8\Delta\omega_I}\sum_{i<j}^{N}(a_{1i}a_{1j}S_z^{(1)} + a_{2i}a_{2j}S_z^{(2)})(I_+^{(i)}I_-^{(j)} + I_-^{(i)}I_+^{(j)}) \tag{1b}$$

$$H_{\Delta} = \frac{1}{16\Delta\omega_I}\sum_{n=1}^{N} a_{1n}^2(S_z^{(1)} - I_z^{(n)}) + a_{2n}^2(S_z^{(2)} - I_z^{(n)}) \tag{1c}$$

where $S^{(1)}$ and $S^{(2)}$ represent the dilute spins (^{15}N and ^{13}C), and I is ^{1}H. $\Delta\omega_I$ is the mismatched Hartmann–Hahn condition that makes the Hamiltonians significant when the mismatch is small. The first term, the recoupling term, recouples two dilute spins by the ^{1}H, and therefore, the ^{1}H dipolar network is used to create couplings among dilute spins. It is this alternative pathway that provides an opportunity to transfer magnetization when the dipolar couplings between dilute spins are weak. The second term, the equilibrating bath term, enables the equilibration of the spin temperature among the spins. For spin diffusion driven by this mechanism [16], ^{15}N spins are polarized to achieve higher spin temperatures, and then, a z-filter is applied to eliminate any residual ^{1}H magnetization that could result in non-selective transfer. Hence, the spin temperature is always higher for the ^{15}N spins, and that drives the magnetization to redistribute to the proton bath and results in decreasing the transfer efficiencies. The third term can be neglected when the lattice sum of each dilute spin is equal; otherwise, the magnetization will be brought to the orthogonal frame according to the commutator. This term could decrease the transfer efficiency in the heteronuclear correlation experiments, because it is difficult to make the lattice sums of ^{13}C and ^{15}N equal to each other. Spin diffusion experiments among ^{15}N in OS solid-state NMR with ^{1}H-irradiation under mismatched Hartmann–Hahn conditions show that even if several different spin dynamics are involved, the recouping term still can assist the magnetization transfers. The Hamiltonians also suggest the feasibility of heteronuclear correlations in triple-resonance experiments on stationary samples. Here we demonstrate ^{13}C-detected HETCOR experiments where the ^{15}N/^{13}C transfer is assisted by ^{1}H-irradiation under mismatched Hartmann–Hahn conditions. In addition, we show that the enhancement of signal intensities and the selectivity depend upon experimental conditions.

2. Results and discussion

Improvement in ^{13}C/^{15}N heteronuclear correlation spectra results from ^{1}H-irradiation under mismatched Hartmann–Hahn conditions. This is demonstrated with two samples under stationary conditions. One sample is a single crystal of ^{15}N, $^{13}C_{\alpha}$ N-acetyl-leucine (NAL), which has four unique molecules in its unit cell. The other sample is selectively ^{15}N, $^{13}C_{\alpha}$ alanine-labeled Pf1 bacteriophage coat protein in magnetically aligned virus particles. There are seven alanine residues in the protein sequence.

One-dimensional ^{13}C and ^{15}N NMR spectra obtained by conventional spin-lock cross-polarization are shown in Fig. 2A and B; the four resolved resonances in each spectrum correspond to the four

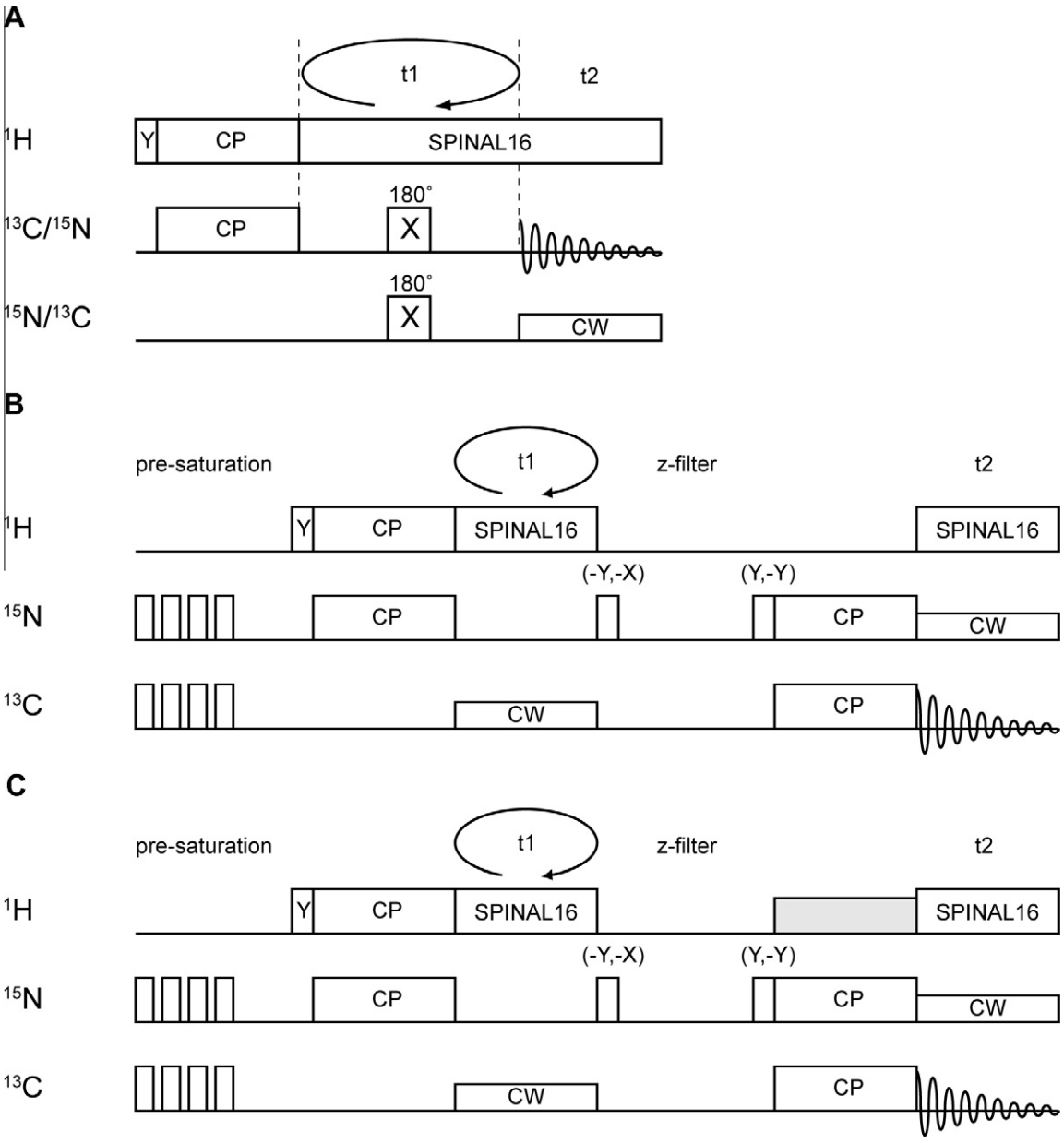

Fig. 1. Timing diagrams for the pulse sequences. (A) ^{15}N–^{13}C dipolar coupling/^{13}C chemical shift or ^{15}N–^{13}C dipolar coupling/^{15}N chemical shift separated-local-field (SLF) experiment. (B) $^{15}N/^{13}C$ HETCOR experiment. (C) $^{15}N/^{13}C$ HETCOR experiment with ^{1}H-irradiation. SLF experiments provide the local fields (dipolar couplings) affecting on the observed spins in the t1 dimension, and the pulse scheme in the t1 dimension can be modified for different demands (^{1}H–^{15}N, ^{1}H–^{13}C, or ^{15}N–^{13}C dipolar couplings). Therefore, the chemical shifts acquired in the t2 dimension can be resolved by these two-dimensional experiments [31,32]. CW refers to continuous wave irradiation and SPINAL-16 [33] refers to the modulation used for heteronuclear decoupling. Pre-saturation is accomplished with thirty 90° pulses separated by 200 μs delay. The z-filter is 5 ms. Mix time for $^{1}H/^{15}N$ cross-polarization is 1 ms, and for $^{15}N/^{13}C$ cross-polarization is 1 ms or 3 ms.

molecular orientations in the unit cell of the single crystal. The ^{15}N–^{13}C heteronuclear dipolar coupling doublets generated in the t1 dimension by the separated-local-field (SLF) experiment using the pulse sequence diagramed in Fig. 1A are shown in Fig. 2C and D. Both the chemical shift and heteronuclear dipolar coupling frequencies depend on the angles between ^{15}N–$^{13}C_\alpha$ bonds and the magnetic field. As a result, the ^{15}N and $^{13}C_\alpha$ sites in a single peptide plane have the same ^{15}N–^{13}C dipolar coupling. By matching the ^{15}N–^{13}C dipolar couplings in the ^{15}N- and ^{13}C-detected ^{15}N–^{13}C dipolar coupling SLF spectra, all four resonances in the ^{15}N and ^{13}C one-dimensional spectra can be correlated. The ^{15}N and $^{13}C_\alpha$ pairs are identified in Fig. 2. The ^{15}N–$^{13}C_\alpha$ dipolar couplings are 200 Hz, 374 Hz, and 451 Hz for pair 2, pair 3 and pair 4, respectively. These doublets show the ^{15}N–^{13}C dipolar couplings are small, as predicted for the peptide system. The ^{15}N–$^{13}C_\alpha$ dipolar coupling of pair 1 is below the resolution limit of this particular experiment, therefore we classify the heteronuclear dipolar coupling of this pair to be ~0 kHz.

The conventional $^{15}N/^{13}C$ HETCOR experiments were performed using the pulse sequence in Fig. 1B. ^{15}N and ^{13}C are pre-saturated to ensure that the magnetization is transferred from other spins without interference from residual magnetization. The magnetization is first transferred from ^{1}H to ^{15}N, and the ^{15}N nuclei then evolve according to their chemical shift interactions by removing heteronuclear dipolar couplings. Subsequently, a 5 ms z-filter is applied to remove any residual ^{1}H magnetization. The first 90° pulse brings the ^{15}N magnetization to the *z*-axis, and is alternated between −Y and −X phase to achieve quadrature detection in the t1 dimension;

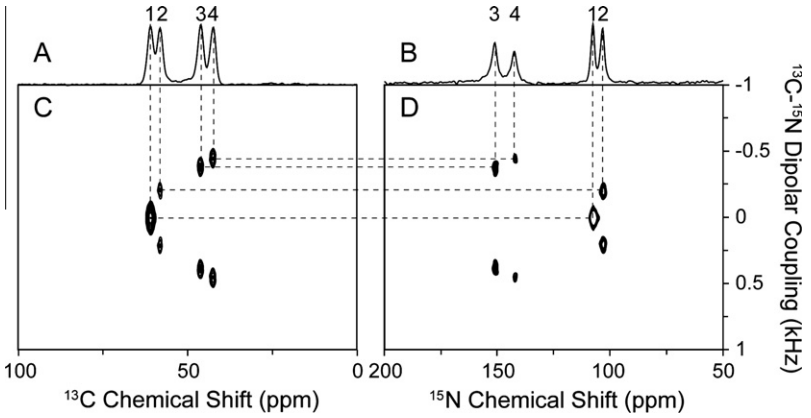

Fig. 2. ^{13}C and ^{15}N chemical shifts correlated by their ^{15}N–^{13}C heteronuclear dipolar couplings in SLF spectra of a ^{15}N, $^{13}C_{\alpha}$ NAL single crystal. (A) ^{15}N decoupled ^{13}C NMR spectrum. (B) ^{13}C decoupled ^{15}N NMR spectrum. (C) ^{13}C-detected ^{15}N–^{13}C heteronuclear dipolar coupling SLF spectra. (D) ^{15}N-detected ^{15}N–^{13}C heteronuclear dipolar coupling SLF spectra. The observed ^{15}N–$^{13}C_{\alpha}$ heteronuclear dipolar couplings are: ~0 Hz (pair 1); 200 Hz (pair 2); 374 Hz (pair 3); and 451 Hz (pair 4).

the second 90° pulse brings the magnetization back, and is alternated between Y and −Y phase to suppress the effects of probe ringing. The magnetization is subsequently transferred with the continuous wave irradiation applied on the ^{15}N and ^{13}C channels simultaneously, and ^{13}C chemical shifts are detected in the t2 dimension. Three resonances shown in Fig. 3A were obtained in the regular ^{15}N/^{13}C HETCOR experiment with 1 ms ^{15}N/^{13}C mixing time. The missing resonance corresponds to resonance 1, which has ~0 kHz ^{15}N–^{13}C dipolar coupling. Notably, no magnetization transfer is observed for pair 1 even with the mixing time extended to 3 ms.

Four resonances are present in Fig. 3B with ^{1}H-irradiation at 40 kHz during the ^{15}N/^{13}C mixing period (Fig. 1B). Slices through all the resonances in the t1 dimension are shown in Fig. 4. The experimental results on the single crystal are fully consistent with the described model: ^{1}H-irradiation provides another pathway to transfer the magnetization from ^{15}N to $^{13}C_{\alpha}$ via the proton bath. The weaker intensities of the pair 2 to pair 4 imply that the other two terms (Eqs. (1b) and (1c)) are involved as well and result in loss of signal intensity. The benefit of ^{1}H-irradiation is shown on pair 1. Although, there are other processes competing with recoupling, the experimental results show that recoupling can drive the magnetization transfer without direct dipolar couplings. Non-selective transfer from the proton bath when ^{1}H-irradiation is applied can be ruled out by inspecting the slices in Fig. 4, since the sharp peaks and flat baselines show only that a specific frequency is transferred.

Recoupling has been shown to assist the ^{15}N/^{13}C transfers when the mismatches are lower than the Hartmann–Hahn condition by 10 kHz. According to the Hamiltonians, the same effect should occur when the mismatch is higher as well. The stronger ^{1}H-irradiation brings the ^{1}H magnetization into the rotating frame more efficiently, and should provide superior recoupling; once the proton bath recouples the dilute spins, all the correlations between ^{15}N and ^{13}C should be observed in the HETCOR spectra. However, we only observed the intra-molecular correlations in the ^{15}N, $^{13}C_{\alpha}$ NAL single crystal sample in the presence of ^{1}H-irradiation at 40 kHz. When the field strength of ^{1}H-irradiation was increased to 60 kHz not only the intra- but also some inter-correlations were observed in the spectra (Fig. 5A). Comparing the spectrum in Fig. 3B, the only difference is the strength of ^{1}H-irradiation, and it shows that the recoupling efficiency is improved by increasing the strength of the B_1 field. All the correlations expected in the unit cell were observed when mixing time was extended to 3 ms (Fig. 5B).

Simulations of the magnetization transfer in a ^{15}N, $^{13}C_{\alpha}$ NAL peptide were carried out using SIMPSON 3.0.1 [27]. To simplify the spin system, only ^{1}H nuclei attached to the ^{15}N, C_{α}, C_{β}, and N-methyl groups were considered, and only the ^{15}N/^{13}C mixing period was simulated to evaluate the transfer efficiency. In the

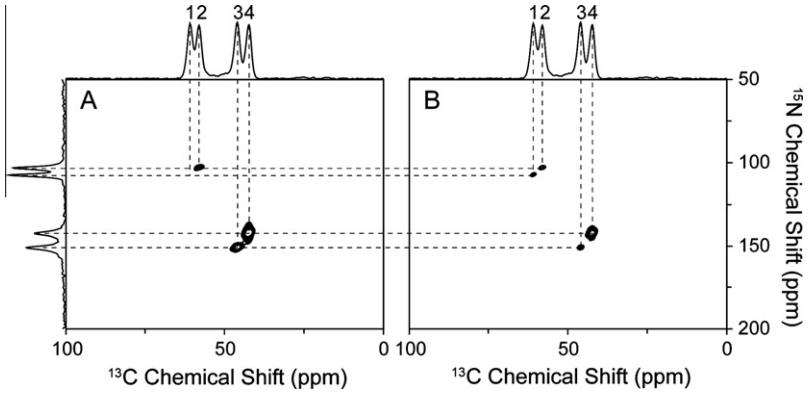

Fig. 3. (A) ^{13}C-detected ^{15}N/^{13}C HETCOR spectrum of a ^{15}N, $^{13}C_{\alpha}$ NAL single crystal. (B) ^{13}C-detected ^{15}N/^{13}C HETCOR with ^{1}H-irradiation at 40 kHz. The one-dimensional spectra aligned on the top and side are the same ^{13}C and ^{15}N CP spectra shown in Fig. 2A and B, respectively. Note in Fig. 3B that the signal from pair 1 is detectable only in the presence of ^{1}H-irradiation. The experiments were performed with 1 ms (shown) and 3 ms ^{15}N/^{13}C mixing time with similar results.

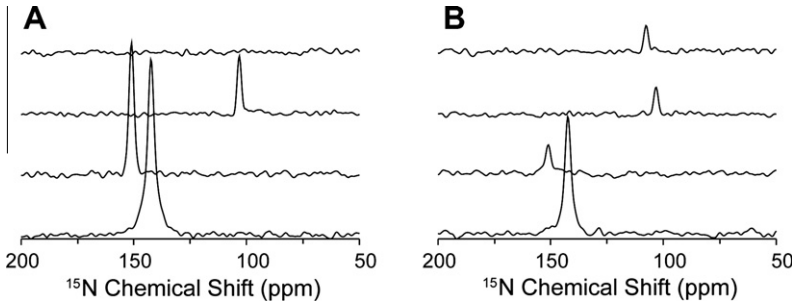

Fig. 4. One-dimensional spectral slices along the ^{15}N chemical shift dimension taken from the two-dimensional spectra shown in Fig. 3. (A) ^{15}N/^{13}C HETCOR. (B) ^{15}N/^{13}C HETCOR with ^{1}H-irradiation at 40 kHz. From top to bottom, the slices correspond to pair 1, pair 2, pair3 and pair 4, respectively. In Fig. 4A, the measured signal-to-noise ratios are 36 (pair 2), 83 (pair 3) and 111 (pairs 4). In Fig. 4B, the measured signal-to-noise ratios are 17 (pair 1), 18 (pair 2), 18 (pair 3) and 74 (pair 4). Reductions in some signal intensities result from competing pathways. The narrow single-line peaks and the flat baselines indicate that the transfer from ^{15}N to ^{13}C is selective.

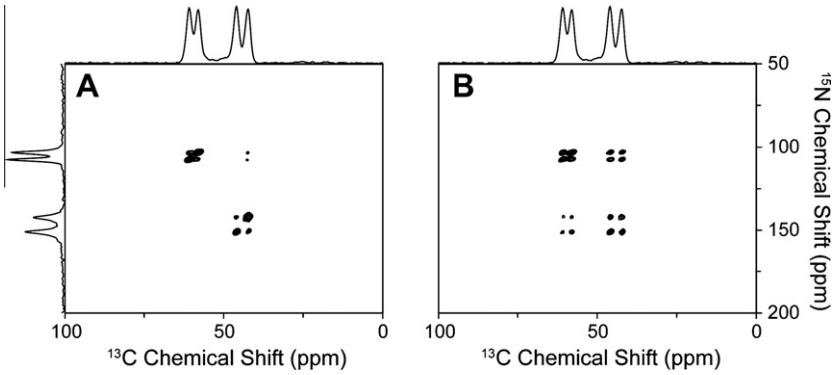

Fig. 5. (A and B) ^{15}N/^{13}C HETCOR spectra obtained with ^{1}H-irradiation of 60 kHz with 1 ms and 3 ms ^{15}N/^{13}C mixing times, respectively, of a ^{15}N, $^{13}C_{\alpha}$ NAL single crystal. One-dimensional spectra on the top and the side are the ^{13}C and ^{15}N CP spectra shown in Fig. 2A and B. Strong inter-molecular correlations in a single crystal are achieved only under the higher mismatched condition.

simulations, a 1 kHz ^{15}N–^{13}C dipolar coupling was utilized. The regular ^{15}N/^{13}C transfer (Fig. 6A) is sensitive to ^{15}N–^{13}C dipolar couplings because they provide the only transfer pathway. The typical CP buildup curve [28] is observed in the simulations when the ^{15}N–^{13}C dipolar coupling is strong; the intensities increase proportionally to the magnitudes of the dipolar couplings, and the dipolar modulation also causes the oscillations in the magnetization buildup curve. The transfer efficiencies are poor when the ^{15}N–^{13}C dipolar couplings are small. However, in the presence of ^{1}H-irradiation (Fig. 6B), no matter the magnitude of the dipolar couplings, they tend to have similar transfer efficiencies. Both higher and lower mismatched conditions (59 kHz and 43 kHz according to the mismatched profile in Fig. 6D) were simulated. The higher field provides better transfer efficiencies, which is consistent with the experimental results shown in Figs. 3B and 5. This demonstrates that the transfer mechanism is dominated by recoupling with the proton bath. The data in Fig. 6C show that transfers for weak ^{15}N–^{13}C dipolar couplings benefit from ^{1}H-irradiation, but that it can decrease the efficiencies for strong ^{15}N–^{13}C dipolar couplings. The mismatched profile (Fig. 6D) was simulated under the small dipolar coupling condition. Two local maxima show up asymmetrically when mismatched conditions are about ±10 kHz, which is similar to the simulations of ^{1}H-irradiation assisted ^{15}N spin diffusion, where the optimal mismatched conditions occur at ±8% [16]. Both the experimental results and simulations suggest that the optimal conditions for ^{1}H-irradiation lie between ±5 kHz and ±15 kHz, mainly depending on the properties of the proton dipolar network. Better transfer efficiency can be observed at the higher mismatch condition because of the larger ^{1}H magnetization in the rotating frame. In practice, the higher mismatched condition drives the inter-peptide correlations that distribute the magnetizations to the proton bath and more distant dilute spins. As a result, the transfer efficiencies would be decreased as shown in Fig. 5.

^{15}N, $^{13}C_{\alpha}$ alanine-labeled Pf1 bacteriophage was used to demonstrate the feasibility for the applications to aligned protein samples. The experiments were performed at a relatively low temperature, to ensure that a single conformation of the protein was present [29]. All the resonances were assigned by comparisons to previous results. Signals from six out of the seven alanine residues were observed with the regular HETCOR experiment (Fig. 7A). A7, A11, and A21 are strong and well resolved. A29 is merged with A21, and A34 and A36 are relatively weak comparing to the other peaks. The signal from A46 is not observed. With ^{1}H-irradiation at a lower mismatched condition of 33.8 kHz, two changes are apparent in the spectrum in Fig. 7B: the signal-to-noise ratio from A34 is increased by 50%, and the signal from A46 can be observed. For the higher mismatched condition at 67.7 kHz, A34 still gains 50% enhancement, while A21 is significantly reduced, which distinguishes between A21 and A29 in Fig. 7C. Other peaks were reduced in intensity in the presence of ^{1}H-irradiation, which serves to reinforce the agreement between the single crystal spectra and simulations. The superimposed spectrum shown in Fig. 7D contains all resonances that are expected from ^{15}N, $^{13}C_{\alpha}$ alanine-labeled Pf1 bacteriophage. Thus by performing multiple experiments with varying strengths of ^{1}H-irradiation, it is possible to detect all ^{15}N/^{13}C correlation peaks from a protein, despite their widely varying magnitudes of heteronuclear dipolar couplings.

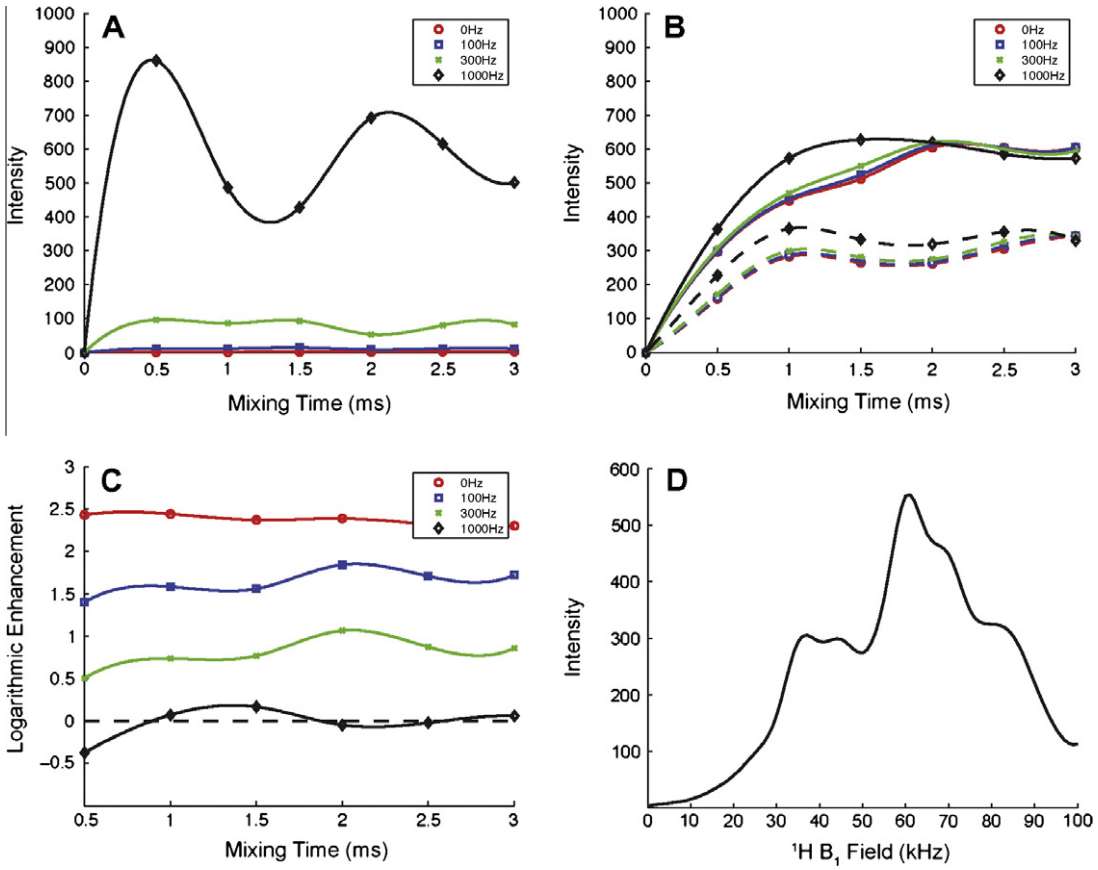

Fig. 6. Simulations of the transfer efficiencies between ^{15}N and ^{13}C with various ^{15}N–^{13}C heteronuclear dipolar couplings. (A) Conventional ^{15}N/^{13}C CP transfer. (B) ^{15}N/^{13}C CP transfer with ^{1}H-irradiation at 59 kHz (solid line) and 43 kHz (dashed line). (C) Logarithmic plot of enhancement by ^{1}H-irradiation. (D) Mismatched profile of ^{1}H-irradiation. (A–C) The ^{15}N–^{13}C$_\alpha$ dipolar couplings were simulated for 0 (red), 100 (blue), 300 (green), 1000 (black) Hz with all other parameters kept the same. The buildup curves were sampled every 500 ms, and the lines connecting the data points show the trends. (D) The simulation was done when ^{15}N–^{13}C$_\alpha$ dipolar coupling equal to zero, and the strength of ^{1}H-irradiation was varied from 0 kHz to 100 kHz. (For interpretation of the references to colour in this figure legend, the reader is referred to the web version of this article.)

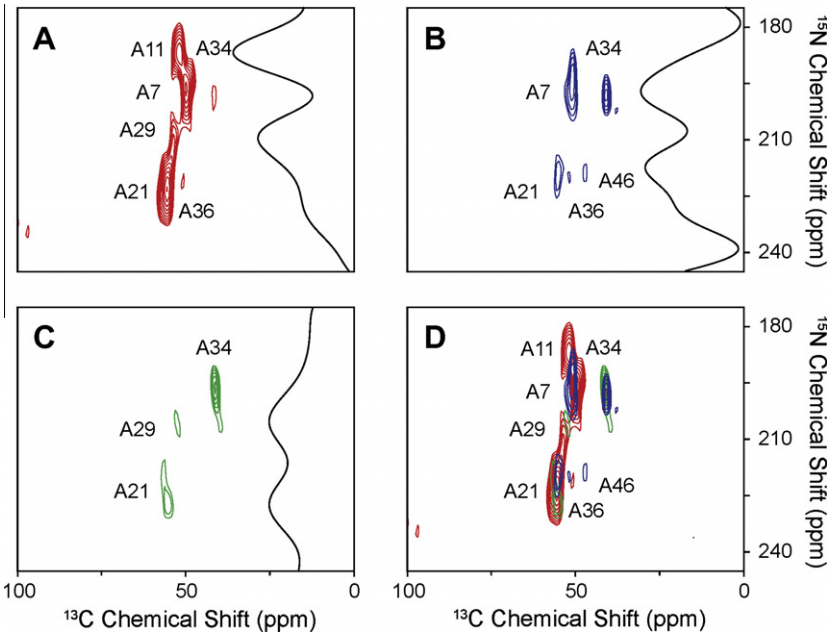

Fig. 7. Two-dimensional ^{15}N/^{13}C HETCOR spectra of selectively ^{15}N, ^{13}C$_\alpha$ alanine-labeled Pf1 bacteriophage that is magnetically aligned in the field. The protein has seven alanine residues. (A) Two-dimensional ^{15}N/^{13}C HETCOR without ^{1}H-irradiation. (B) Two-dimensional ^{15}N/^{13}C HETCOR with ^{1}H-irradiation at 33.8 kHz. (C) Two-dimensional ^{15}N/^{13}C HETCOR with ^{1}H-irradiation at 67.7 kHz. The slices shown in panels A, B, and C were taken at 53.7 ppm in the ^{13}C chemical shift dimension, corresponding to the resonance from A29. (D) This spectrum is a superposition of the spectra in panels A (red), B (blue), and C (green); it displays all of the ^{15}N/^{13}C correlations in the selectively ^{15}N-alanine-labeled Pf1 bacteriophage, and demonstrates the possibility of observing all ^{15}N/^{13}C correlations regardless of the strength of their heteronuclear dipolar couplings by obtaining spectra under several different transfer conditions. (For interpretation of the references to colour in this figure legend, the reader is referred to the web version of this article.)

3. Conclusions

^{13}C-detected triple-resonance experiments can detect all ^{15}N/^{13}C correlation resonances with high sensitivity, as long as they are performed with ^{13}C-detection under several different conditions of ^{1}H radiofrequency irradiations. The frequencies of the ^{15}N/^{13}C correlation resonances provide valuable constraints for the calculation of protein structures in OS solid-state NMR. Moreover, ^{15}N/^{13}C transfers can be used as a filter to eliminate interference from natural abundance signals from the lipids [18]. ^{1}H-irradiation under mismatched Hartmann–Hahn conditions assists magnetization transfer from ^{15}N to ^{13}C. The experimental results obtained on single crystal and aligned protein samples, and simulations demonstrate the validity of this recoupling mechanism. The transfer mechanism relies primarily on the ^{1}H dipolar network, which is well suited for OS solid-state NMR experiments. The spin dynamics are complex once the spins are recoupled by ^{1}H-irradiation, and therefore, some of the transfer efficiencies may be lost, especially when the ^{15}N–^{13}C dipolar couplings are large. However, this method is complementary to other procedures especially because it provides good transfer efficiencies for small ^{15}N–^{13}C dipolar couplings. Both mismatched conditions are used in order to enhance the intensities of signals with different dipolar couplings. Combined with conventional spin-lock CP transfer, these experiments have the potential to simultaneous measure all of the ^{13}C and ^{15}N chemical shift frequencies and correlate proximate residues in a protein, which provides the basis for systematic assignment schemes.

4. Methods

4.1. ^{15}N, $^{13}C_\alpha$ NAL single crystal spectra

The NMR experiments were performed on a Varian Inova spectrometer with ^{1}H, ^{13}C, and ^{15}N frequencies of 500.125 MHz, 125.76 MHz, and 50.68 MHz, respectively. A home-built modified Alderman Grant coil (MAGC) triple-resonance probe [19], which was designed for lossy biological samples, was used for these experiments. All the spectra were obtained at room temperature. The ^{1}H carrier frequency was set at 4.7 ppm; the ^{13}C carrier frequency was set at 54.94 ppm; and the ^{15}N carrier frequency was set at 79.26 ppm. ^{13}C- and ^{15}N-detected spectra were acquired with 512 and 1024 complex points in the direct dimensions, respectively. CP spectra were acquired with 64 scans and 40 μs dwell time. ^{15}N–^{13}C dipolar coupling SLF spectra were acquired with 4 scans, 100 μs dwell time and 96 points in the indirect dimension, and 40 μs dwell time in the direct dimension. HETCOR spectra were acquired with 4 scans, 100 μs dwell time and 192 complex points in the indirect dimension, and 40 μs dwell time and 512 complex points in the direct dimension. The mixing time for ^{1}H/^{15}N and ^{1}H/^{13}C CP was 1 ms, and ^{15}N/^{13}C CP was 1 ms or 3 ms. For all the experiments the recycle delay was 6 s. Pre-saturation consisted of thirty 90° pulses separated by 200 μs, and the z-filter delay was 5 ms. The strength of the continuous wave decoupling on ^{15}N and ^{13}C channels was 40 kHz, and all other irradiations were performed at 50 kHz, except for the variable ^{1}H-irradiation during the ^{15}N/^{13}C mixing period. The experimental data were zero filled to 512 and 1024 data points in the indirect and direct dimensions, respectively, and were multiplied by a sine bell window function prior to Fourier transformation.

4.2. ^{15}N, $^{13}C_\alpha$ alanine-labeled Pf1 bacteriophage spectra

The Pf1 filamentous bacteriophage sample was prepared as described previously [30]. The final bacteriophage sample was diluted to 40 mg/ml with sodium borate buffer (pH = 8), and the final volume was 150 μl. The spectra were obtained at −2 °C to ensure that the coat protein was in its 'low temperature' conformation. The ^{1}H carrier frequency was set at 4.7 ppm; the ^{13}C carrier frequency was set at 100 ppm, and the ^{15}N carrier frequency was set at 213 ppm. HETCOR spectra were acquired with 400 scans, 100 μs dwell time, 32 complex points in the indirect dimension, and 25 μs dwell time and 256 complex points in the direct dimension. Mixing time of ^{1}H/^{15}N CP was 1 ms and ^{15}N/^{13}C CP was 3 ms. The recycle delay was 4 s. All other conditions were the same as described above for the single crystal.

4.3. Simulations

Only the ^{15}N/^{13}C mixing period was simulated to evaluate the transfer efficiency. The simulations were carried out with SIMPSON 3.0.1. The model was based on the single crystal structure [16]; however, the spin system was simplified to ^{15}N, $^{13}C_\alpha$, the ^{1}H attached to the N, C_α, C_β, and N-methyl group. Euler angles "β" in the input file were manually adjusted to 90° for ^{1}H–^{15}N, ^{1}H–$^{13}C_\alpha$ and ^{15}N–$^{13}C_\alpha$ dipolar couplings, and therefore, the dipolar couplings can be varied without angular considerations. For all the simulations, ^{1}H–^{15}N and ^{1}H–$^{13}C_\alpha$ dipolar couplings were 12.18 and 22.80 kHz according to the bond lengths. ^{15}N–$^{13}C_\alpha$ dipolar couplings were adjusted manually according to each case. ^{15}N/^{13}C mixing period was 3 ms for the mismatched profile simulation.

Acknowledgments

We thank C.H. Wu and B.B. Das for helpful discussions. This research was supported by Grants from the National Institutes of Health, and it utilized the Biomedical Technology Resource for NMR Molecular Imaging of Proteins at the University of California San Diego, which is supported by Grant P41EB002031.

References

[1] F.M. Marassi, C. Ma, H. Gratkowski, S.K. Straus, K. Strebel, M. Oblatt-Montal, M. Montal, S.J. Opella, Correlation of the structural and functional domains in the membrane protein Vpu from HIV-1, Proc. Natl. Acad. Sci. U.S.A. 96 (1999) 14336–14341.
[2] S.H. Park, S. Prytulla, A.A. De Angelis, J.M. Brown, H. Kiefer, S.J. Opella, High-resolution NMR spectroscopy of a GPCR in aligned bicelles, J. Am. Chem. Soc. 128 (2006) 7402–7403.
[3] A.A. De Angelis, S.C. Howell, A.A. Nevzorov, S.J. Opella, Structure determination of a membrane protein with two trans-membrane helices in aligned phospholipid bicelles by solid-state NMR spectroscopy, J. Am. Chem. Soc. 128 (2006) 12256–12267.
[4] G.A. Cook, S.J. Opella, NMR studies of p7 protein from hepatitis C virus, Eur. Biophys. J. 39 (2009) 1097–1104.
[5] S.J. Opella, A.C. Zeri, S.H. Park, Structure, dynamics, and assembly of filamentous bacteriophages by nuclear magnetic resonance spectroscopy, Annu. Rev. Phys. Chem. 59 (2008) 635–657.
[6] M.J. Baryro, T. Maly, N.R. Birkett, C.E. Bacphee, C.M. Dobson, R.G. Griffin, High-resolution MAS NMR analysis of PI3-SH3 amyloid fibrils: backbone conformation and implications for protofilament assembly and structure, Biochemistry 49 (2010) 7474–7484.
[7] A.A. De Angelis, A.A. Nevzorov, S.H. Park, S.C. Howell, A.A. Mrse, S.J. Opella, High-resolution NMR spectroscopy of membrane proteins in aligned bicelles, J. Am. Chem. Soc. 126 (2004) 15340–15341.
[8] N. Tjandra, A. Bax, Direct measurement of distances and angles in biomolecules by NMR in a dilute liquid crystalline medium, Science 278 (1997) 1111–1114.
[9] T.A. Cross, J.A. DiVerdi, S.J. Opella, Strategy for nitrogen NMR of biopolymers, J. Am. Chem. Soc. 104 (1982) 1759–1761.
[10] C. Wu, A. Ramamoorthy, S. Opella, High-resolution heteronuclear dipolar solid-state NMR spectroscopy, J. Magn. Reson. A109 (1994) 270–272.
[11] A.A. Nevzorov, S.J. Opella, A "magic sandwich" pulse sequence with reduced offset dependence for high-resolution separated local field spectroscopy, J. Magn. Reson. 164 (2003) 182–186.
[12] C.H. Wu, S.J. Opella, Proton-detected separated local field spectroscopy, J. Magn. Reson. 190 (2008) 165–170.
[13] C.H. Wu, S.J. Opella, Shiftless nuclear magnetic resonance spectroscopy, J. Chem. Phys. 128 (2008) 052312.

[14] M.F. Mesleh, G. Veglia, T.M. DeSilva, F.M. Marassi, S.J. Opella, Dipolar waves as NMR maps of protein structure, J. Am. Chem. Soc. 124 (2002) 4206–4207.
[15] F.M. Marassi, S.J. Opella, A solid-state NMR index of helical membrane protein structure and topology, J. Magn. Reson. 144 (2000) 150–155.
[16] A.A. Nevzorov, Mismatched Hartmann–Hahn conditions cause proton-mediated intermolecular magnetization transfer between dilute low-spin nuclei in NMR of static solids, J. Am. Chem. Soc. 130 (2008) 11282–11283.
[17] N.J. Traaseth, T. Gopinath, G. Veglia, On the performance of spin diffusion NMR techniques in oriented solids: prospects for resonance assignments and distance measurements from separated local field experiments, J. Phys. Chem. B 114 (2010) 13872–13880.
[18] N. Sinha, F.V. Filipp, L. Jairam, S.H. Park, J. Bradley, S.J. Opella, Tailoring 13C labeling for triple-resonance solid-state NMR experiments on aligned samples of proteins, Magn. Reson. Chem. 45 (Suppl. 1) (2007) S107–115.
[19] E.C. Lin, C.H. Wu, Y. Yang, C.V. Grant, S.J. Opella, 1H–13C separated local field spectroscopy of uniformly 13C labeled peptides and proteins, J. Magn. Reson. 206 (2010) 105–111.
[20] A. Pines, M.G. Gibby, J.S. Waugh, Proton-enhanced nuclear induction spectroscopy. A method for high-resolution NMR of dilute spins in solids, J. Chem. Phys. 56 (1972) 1776–1777.
[21] A. Pines, M. Gibby, J. Waugh, Proton enhanced NMR of dilute spins in solids, J. Chem. Phys. 59 (1973) 569–590.
[22] J. Schaefer, R.A. McKay, E.O. Stejskal, Double-cross-polarization NMR of solids, J. Magn. Reson. 34 (1979) 443–447.
[23] A. Ramamoorthy, C.H. Wu, S.J. Opella, Three-dimensional solid-state NMR experiment that correlates the chemical shift and dipolar coupling frequencies of two heteronuclei, J. Magn. Reson. B107 (1995) 88–90.
[24] A.A. Nevzorov, S.H. Park, S.J. Opella, Three-dimensional experiment for solid-state NMR of aligned protein samples in high field magnets, J. Biomol. NMR 37 (2007) 113–116.
[25] J. Xu, R. Soong, S.-C. Im, L. Waskell, A. Ramamoorthy, INEPT-based separated-local-field NMR spectroscopy: a unique approach to elucidate side-chain dynamics of membrane-associated proteins, J. Am. Chem. Soc. 132 (2010) 9944–9947.
[26] J.R. Lewandowski, G. De Paëpe, R.G. Griffin, Proton assisted insensitive nuclei cross polarization, J. Am. Chem. Soc. 129 (2007) 728–729.
[27] M. Bak, J. Rasmussen, N. Nielsen, SIMPSON: a general simulation program for solid-state NMR spectroscopy, J. Magn. Reson. 147 (2000) 296–330.
[28] L. Müller, A. Kumar, T. Baumann, R.R. Ernst, Transient oscillations in NMR cross-polarization experiments in solids, Phys. Rev. Lett. 32 (1974) 1402.
[29] D.S. Thiriot, A.A. Nevzorov, S.J. Opella, Structural basis of the temperature transition of Pf1 bacteriophage, Protein Sci. 14 (2005) 1064–1070.
[30] D.S. Thiriot, A.A. Nevzorov, L. Zagyanskiy, C.H. Wu, S.J. Opella, Structure of the coat protein in Pf1 bacteriophage determined by solid-state NMR spectroscopy, J. Mol. Biol. 341 (2004) 869–879.
[31] J.S. Waugh, Uncoupling of local field spectra in nuclear magnetic resonance: determination of atomic position in solids, Proc. Natl. Acad. Sci. U.S.A. 73 (1976) 1394–1397.
[32] N. Sinha, C.V. Grant, S.H. Park, J.M. Brown, S.J. Opella, Triple resonance experiments for aligned sample solid-state NMR of (13)C and (15)N labeled proteins, J. Magn. Reson. 186 (2007) 51–64.
[33] N. Sinha, C.V. Grant, C.H. Wu, A.A. De Angelis, S.C. Howell, S.J. Opella, SPINAL modulated decoupling in high field double- and triple-resonance solid-state NMR experiments on stationary samples, J. Magn. Reson. 177 (2005) 197–202.